Spectral Confirmation of a 80 Mpc Filament of Galaxies at Redshift 2.38

Paul J. Francis[1]

Research School of Astronomy and Astrophysics, the Australian National University, Canberra 0200, Australia

pfrancis@mso.anu.edu.au

Povilas Palunas

McDonald Observatory, University of Texas, Austin, TX 78712

Harry I. Teplitz

SIRTF Science Center, California Institute of Technology, Mail Code 100-22, 770 South Wilson Avenue, Pasadena, CA 91125

Gerard M. Williger

Dept. of Physics and Astronomy, Johns Hopkins University, 3701 San Martin Drive, Baltimore, MD 21218

and

Bruce E. Woodgate

NASA Goddard Space Flight Center, Code 68, Greenbelt, MD 20771

Received _____; accepted _____

[1]Joint Appointment with the Department of Physics, Faculty of Science, the Australian National University

ABSTRACT

The existence of an 80 co-moving Mpc filament of galaxies at redshift 2.38 is confirmed. Palunas et al. (2004) originally identified this filament as an apparent alignment of candidate Lyα emitting galaxies. The 2dF multi-fibre spectrograph on the Anglo-Australian Telescope was used to obtain spectral confirmation for 27 of the candidate galaxies, and one QSO that lies within the filament. Redshifts were also obtained for many foreground galaxies and QSOs. A large and highly significant cluster of ten QSOs was found at $z = 1.65$.

We demonstrate that either line width or the absence of other emission lines can be used to discriminate between Lyα emission from high redshift galaxies and [O II] from foreground dwarf galaxies.

Subject headings: Large-scale structure of universe — galaxies: clusters — galaxies: high redshift — quasars: general

1. Introduction

A large fraction of galaxies today lie in filamentary structures, such as the Great Wall (Geller & Huchra 1989), separated by voids. When did these structures form? There are now some tentative observations suggesting that this topology was already in place as early as redshift three (eg. Campos et al. 1999; Møller & Fynbo 2001).

The largest scale survey to claim the detection of filaments and voids at high redshifts was that of Palunas et al. (2004). They searched for candidate Lyα emitting galaxies in an 80$\times$ 80 $\times$ 60 co-moving Mpc region. The region was imaged through a narrow-band (54Å) filter, centred at 4110Å. This was sensitive to Lyα emitting galaxies at $z \sim 2.38$. 39 candidate galaxies were found.

These candidate $z \sim 2.38$ galaxies mostly lie in a filamentary structure, over 80 co-moving Mpc in length. This filament is seemingly bracketed by voids on both sides. Palunas et al. (2004) argue that this structure is statistically significant, and that that the size of the voids and the filament is larger than would be expected from CDM (Cold Dark Matter) simulations.

Palunas et al. (2004) did not, however, have spectra of their candidate high redshift galaxies. It was thus possible that some or all of them were actually foreground galaxies: galaxies lying at $z \sim 0.1$ whose O II 3727Å line lies within the filter bandpass. Even if they were Lyα emitting galaxies at $z \sim 2.38$, their observations only constrained the two dimensional position of the galaxies and not their precise redshift.

Spectral confirmation of these galaxies was clearly desirable, but was technically challenging, due to the faintness of the sources and the large region of the sky over which they were spread. In this paper, we present confirmation spectrscopy of these galaxy candidates, obtained using a wide-field fibre spectrograph.

2. Observations and Reduction

Our spectroscopic confirmation was carried out using the 2dF multi-fibre spectrograph on the Anglo-Australian Telescope (AAT, Lewis et al. 2002). This spectrograph has 400 fibers, spread over a circular field of radius one degree, located at the prime focus of the AAT. This field is more than enough to allow us to observe all our candidates simultaneously.

2.1. Fiber Allocation

Fibers were allocated to targets using the *configure* program (Lewis et al. 2002). First priority in the fibre allocation was given to the candidate z=2.38 galaxies identified by Palunas et al. (2004) (the main sample). We were able to allocate fibres to all but two of these (the two unobserved sources, those at 21:40:33.1 -44:36:10.8 and 21:43:05.9 -44:27:21.0, J2000, lay too close to other candidate galaxies for fibre allocation). Second priority was 26 brighter point sources which also showed excess narrow-band flux: these were potential z=2.38 QSOs. Three of these were too bright for us to observe, but we were able to allocate fibres to twenty of the remaining twenty-three (the point source sample).

The candidate list of Palunas et al. (2004) only included sources with excess narrow-band emission of equivalent width > 125Å. This was done to minimise contamination from foreground [O II] emitting galaxies, but may also have eliminated some Lyα emitting sources. To check this, we selected a sample of 86 sources which showed excess emission in the narrow band, but not enough to meet this equivalent width threshold (the low equivalent width sample). We were able to allocate fibres to 70 of these sources.

211 UVX sources were selected, as possible foreground QSOs. We were able to allocate fibres to 120 of these (the UVX sample). Four candidate color-selected high redshift QSOs were also observed.

Fibres were allocated to 17 Chandra sources: these will be discussed by Williger et al (in preparation).

2.2. Observations

Observations were carried out on the nights of 2003 August 31 and September 1. Conditions were poor: the first night was mostly cloudy, and the second night, while clear,

suffered from typical 2.5″ seeing. We obtained a total integration time of 5400 sec on the first night and 32,400 sec on the second night, though much of this was obtained at high airmass, or while the moon was up.

The first night's data were reduced quickly, allowing us to identify several foreground galaxies amongst the low equivalent width sample. The fibre configuration was changed for the second night by eliminating these sources, allowing us to observe more of the various lower priority samples. This also means that the higher priority sources were observed through different fibres on the different nights, giving us a check against systematic errors.

We used the 600V gratings in both the 2dF spectrographs, centered at a wavelength of 4982Å. This gave a spectral resolution of 450 km s^{-1} and a wavelength range of 3890 – 6080Å. The data were reduced using the *2dfdr* software (Lewis et al. 2002).

Spectra from each night were co-added separately, as a check on the reality of any faint features seen. A weighted sum of the spectra from both nights was then used in the final analysis.

2.3. Spectral Classification

All spectra were classified interactively. For sources showing a single narrow emission line at $\sim$ 4110Å, we classified them either as $z \sim 2.38$ Lyα emitting galaxies or $z \sim 0.1$ [O II] blue compact galaxies using the following criteria:

- If we see corresponding [O III] and/or Hβ emission lines, we identify the source as an [O II] emitting galaxy at $z \sim 0.1$.
- If we see corresponding C IV emission line, we identify the source as a Lyα emitting galaxy at $z \sim 2.38$.

- If the ~ 4110Å line has a velocity width > 500km s^{-1}, and no other lines are seen, we classify the line as Lyα at $z \sim 2.38$, on the basis that the [O II] emission of a blue compact galaxy is unlikely to be this broad.

- The remaining three sources (with single narrow lines) are classified as Lyα emitting galaxies at $z \sim 2.38$, on the basis that had they been as $z \sim 0.1$, we should have easily seen [O II] emission (§ 4.4). One of these three was confirmed by Francis, Woodgate & Danks (1997) to lie at $z \sim 2.38$.

The detection of an emission-line is regarded as secure if it is seen at greater than 5σ confidence. If seen between 3 and 5 σ confidence, it is regarded as marginal.

3. Results

3.1. The Main Sample

We obtain secure spectral confirmation that 14 of the 37 observed sources in the main sample, and one additional source from the low equivalent width sample, are indeed Lyα emitting galaxies at $z \sim 2.38$. Three of these have previous spectral confirmation (Francis, Woodgate & Danks 1997). These spectra are shown in Fig 1, and their properties are listed in Table 1.

A further 12 main sample sources show a weaker ($3 - 5$ σ) emission line: we consider these to be marginally confirmed. We checked that the lines we marginally see are not [O II] by co-adding all these marginal sources, redshifted to align the putative Lyα lines. No sign of [O III] emission was seen in the coadded spectrum. These marginal spectra are shown in Fig 2 and listed in Table 2.

One further source (21 41 07.38 -44 38 11.7) showed clear stellar absorption and

is hence a foreground source. In the remaining six sources, no significant emission or absorption features were seen anywhere in the spectra.

The spectra for which we obtained secure spectral classification are predominatly the brighter and/or higher surface brightness sources: we get a secure spectral confirmation of 62% of sources with narrow-band magnitudes brighter than NB = 22.6, but for only 40% of the fainter sources. Had these fainter sources been foreground $z \sim 0.1$ sources, we would easily have seen their [O III] emission, as it is usually stronger than [O II] and lies at a wavelength where our sensitivity is good (§ 4.4). We therefore consider it probable that the majority of the fainter sources are indeed at z=2.38, but that longer exposure times and/or better weather would be needed to get spectral confirmation.

One source, B5 (coordinates 21:43:03.57 -44:23:44.2, J2000), proved impossible to classify. B5 is one of the most luminous narrow-band excess sources, and Palunas et al. (2004) classified it as a Lyα blob. Their image of it shows a point source surrounded by diffuse fuzz. Our spectrum (Fig 4) shows two clear broad emission lines: one at 4110Å and the other at 5930Å. Both lines, though noisy, are independently seen in the coadded data from each night, and must therefore be regarded as secure. A more marginal candidate broad line is possibly seen at 4440Å. The breadth of the lines ($\sim$ 4000km s^{-1}) clearly indicates that this is a QSO. The fact that B5 shows extended narrow-band fuzz suggests that the line at 4110Å is either Lyα or [O II]. If the former, however, the 5930Å line would have a rest-frame wavelength of $\sim$ 1750Å, which does not correspond to any normal QSO emission line (Francis et al. 1991). If the latter, we do not see any Balmer lines or [O III], and the 5930Å line would lie at rest-frame 5390Å; another wavelength which does not correspond to any strong QSO line. No alternative identification of the lines works any better. A higher quality spectrum with wider wavelength coverage is clearly needed.

3.2. QSOs

Thirteen of the twenty point source sample objects observed were QSOs with a broad emission line within the narrow-band filter bandpass. Only one of these (Fig 3) was at the filament redshift: ten lie at $z \sim 1.65$ which places C IV within the passband. The other two lie at z=0.457 and z=1.458, placing Mg II and He II respectively in the passband. Two of the remaining sources had no significant features in their spectra, and the other two were low redshift compact emission-line galaxies (one with [O II] in the passband).

A further 41 QSOs were found in the UVX sample, and three in the low equivalent width sample. Three of the UVX QSOs lie at higher redshifts than our candidate filament, and are shown in Fig 3. All QSOs identified are listed in Table 3. Given our restricted wavelength coverage, we often see only a single emission line: these one line sources are noted in the table, and given redshifts typically assuming that this line is Mg II. QSOs with lines only marginally detected are indicated with question marks.

3.3. Foreground Galaxies

We detect 19 galaxies whose redshifts place [O II] within the passband of our filter. These, together with other foreground emission-line galaxies, are listed in Table 4.

4. Discussion

4.1. Is the Filament Real?

In Fig 5 we show the distribution of confirmed $z = 2.38$ galaxies. Note that they are spread quite uniformly amongst the candidates on the sky, and trace the same filamentary distribution.

Could there be a substantial population of foreground contaminants amongst the marginal sources? Fig 6 shows that the confirmed foreground [O II] emitting galaxies have a very different distribution, concentrated on the cluster Abell 3800 (Abell, Corwin & Olowin 1989). The lack of [O III] emission in the coadded marginal spectra (§ 3.1) is further evidence that the bulk of these cannot be foreground sources. Of the 16 main sample sources with secure spectral classifications, 15 lie at the filament redshift: if the same fraction applies to the fainter sources, ~ 35 of the 38 will lie at this redshift.

We therefore tentatively conclude that the filament is real, and that at least 50% of the galaxies within it, and probably much more, really are Lyα emitting sources at $z \sim 2.38$.

4.2. Is it a filament or a sheet?

The distribution of Lyα redshifts is shown in Fig 7. The mean redshift (including both secure and marginal candidates) is $z = 2.3791$, with a standard deviation of 820km s^{-1}. The corresponding figures for sources with secure redshifts only are $z = 2.3807$ and 800km s^{-1}. There is no significant correlation between position on the sky and measured redshift.

Are we really seeing a concentration of sources at a particular wavelength, or is the measured wavelength dispersion simply an artefact of the bandpass of our selection filter? Fig 7 suggests that the observed redshift distribution is more sharply peaked than the filter bandpass, and that the peak lies at a slightly longer wavelength. We tested this by Monte-Carlo simulating samples of randomly distributed galaxies observed through this filter, assuming a Lyα luminosity function with $N(l) \propto L^{-0.87}$, as used by Palunas et al. (2004). Fewer than 0.1% (0.6% for secure sources only) of the simulations has measured velocity dispersions as low as we obtained.

The statistical difference is mostly driven by the relative lack of observed lines lying

in the wavelength range 4085 — 4105Å: ie. the observed galaxy distribution has a lower redshift cut-off. But does it have a higher redshift cut-off, or is the lack of observed galaxies with Lyα wavelengths onger than around 4125Å caused only by the filter bandpass? Once again, we tested this using our Monte-Carlo simulations. Fewer than 1% of simulations having the same sample size as the combined secure and marginal samples had as few sources longward of 4125Å as we saw, but if we restrict ourselves to sources with secure spectral classifications only, this fraction rises to 10%.

We conclude that we are probably looking at a filament viewed from sideways, rather than an edge-on sheet. There remains a small possibility that it is a sheet but that we are only sampling its front edge, as we do not definitively detect a higher redshift cut-off.

Taken at face value, our measured velocity dispersion of $\sim$ 800km s^{-1} would imply that we are looking at a very massive cluster, or a structure significantly extended along the line of sight. We note, however, that the measured velocity dispersion is comparable to the average velocity widths of the Lyα line in the individual galaxies (median 830km s^{-1} full width at half maximum height). As Lyα is expected to be enormously optically thick, one might expect the emerging line to be offset from the true velocity by of order the velocity dispersion of that galaxy. Thus the measured velocity dispersion should be taken as an upper limit: measuring the true value and the three dimensional structure of the filament will require observations in a line less optically thick.

4.3. QSO Clusters

Only one QSO was found at the filament redshift: would we have expected more? We are effectively finding QSOs down to $B \sim 21.8$. Extrapolating the QSO luminosity functions of Boyle et al. (2000), and allowing for QSOs to be selected in our narrow-band

filter even if only part of their broad Lyα emission is within the filter bandpass, we would expect 0.75 QSOs to have been found, if the region studied was not overdense in them. Thus the observations are quite consistent with this region being average.

Palunas et al. (2004) reported that the filament region had an overdensity of Lyα emitting galaxies of 5.8 ± 2.5. Is this consistent with the observation of only one QSO? Using Poisson statistics, if the region were overdense by a factor of 5.8, we'd find only one QSO 7% of the time. If the overdensity were only 3.3, this rises to 29%. Thus finding only one QSO is consistent with such an overdensity, though favouring lower values.

Perhaps the greatest surprise is the 10 QSOs identified with $1.61 < z < 1.69$, which places some or all of their C IV emission in the narrow-band filter. From the Boyle et al. (2000) luminosity functions, we'd predict only 1.8 QSOs in this range. The Poisson probability of finding 10, if the field were not overdense, is only 0.5%. We therefore conclude that a cluster of QSOs lies in the foreground of our field at $z = 1.65$.

In Fig 8 we show the distribution of these QSOs. It is clearly non-random: they are concentrated into the South-East corner of the field. The overdensity of QSOs within this region is > 3 with 95% confidence.

Could gravitational lensing by this cluster, plus Abell 3800, be responsible for the filament and voids seen at z=2.38? Cluster lensing could certainly be amplifying a handfull of individual sources, but expected magnifications over the enormous extent of our field are insignificant.

4.4. Discriminating between high-z galaxies and foreground blue compact galaxies.

All searches for Lyα emitting galaxies have the problem of eliminating foreground line contamination. Due to the multi-object capability of 2dF, we are in the unusual position of having spectra of both a large sample of Lyα emitting galaxies and of foreground [O II] emitting galaxies, allowing us to compare their properties and test various possible selection criteria.

Fig 9 shows the distribution of confirmed Lyα emitting galaxies and of confirmed foreground [O II] emitting galaxies as a function of color excess and magnitude. The sources are clearly separated in this plane: our spectroscopy of the low equivalent width sample only identified one clear Lyα emitting galaxy (there are two more rather marginal candidates).

At first glance, this is surprising, as Lyman-dropout selected samples (eg. Steidel et al. 2000) show us that low equivalent width Lyα emitting galaxies must be plentiful. The lack of such galaxies in our sample is probably, however, a selection effect. As Fig 9 shows, we did not observe faint sources with small B-NB colors. They were omitted from our spectroscopic target list because the narrow-band excess in this sample is not statistically significant. Unfortunately, it is precisely in this region of the figure that our Lyα emitting galaxies would lie, were their emission-line equivalent widths narrower.

Once spectra have been obtained, how can we best discriminate against foreground galaxies? Line width is one possibility: 12/16 of our securely classified Lyα emitting galaxies had clearly resolved spectral line widths, at our 450km s^{-1} resolution (Table 1). This likely underestimates the fraction of sources with resolvable lines, as broad lines are harder to detect in our low signal-to-noise ratio spectra. One of the remaining sources (B2) is confirmed to lie at $z = 2.38$ by the detection of C IV emission by /citetfra97.

C IV is normally too faint to be seen in our data, and so seldom provides a useful discriminant. Luckily, the [O III] (5007Å) line is usually strong in foreground galaxies (Fig 10). The median ratio of the [O III] 5007Å line to [O II] 3727Å is 1.7, and none of our foreground galaxies show ratios of less than 0.5. Hβ is also often seen, but is usually weaker than [O II]. Could the lack of galaxies with low ratios of [O III] to [O II] be caused by us misclassifying such sources as Lyα emitters? Only two sources classified as Lyα emitters show neither C IV emission or a broad Lyα line: if they were O II emitting galaxies at $z \sim 0.1$, the inferred 3σ upper limits on [O III]/[O II] are 0.21 and 0.35. It is thus possible that there is a tail of [O II] emitting galaxies with very weak [O III] and Hβ, but such galaxies comprise at most $\sim 10\%$ of the foreground population.

We conclude that both line width and the absence of [O III] emission provide fairly effective discrimination between Lyα and [O II] emitting galaxies.

5. Conclusions

We conclude that galaxy candidates identified by Palunas et al. (2004) are indeed mostly Lyα emitting galaxies at $z \sim 2.38$. The filament and voids that they identified are thus real. We also tentatively conclude that the filament, seen in projection, is indeed a two-dimensional structure, and not a slice through some three dimensional sheet.

Curiously, the filament region is not overdense in QSOs, but we find a highly significant cluster of foreground QSOs at $z \sim 1.65$. One QSO was found lying within the filament, as were three background QSOs. Follow-up spectroscopy of these QSOs may allow us to constrain the gas within the filament and voids, as has already been done for the three background QSOs previously known (Francis & Williger 2004).

We show that either the width of the Lyα emission line or the absence of other lines

can be an effective tool for discriminating against foreground [O II] emitting galaxies.

This study was funded by a NASA grant NRA–98–03–UVG–011, and supported by the STIS IDT through the National Optical Astronomical Observatories and by the Goddard Space Flight Center.

REFERENCES

Abell, G.O., Corwin, H.G. & Olowin, R.P. 1989, ApJS, 70, 1

Boyle, B.J., Shanks, T., Croom, S.M., Smith, R.J., Miller, L., Loaring, N. & Heymans, C. 2000, MNRAS, 317, 1014

Campos, A., Yahil, A., Windhorst, R.A., Richards, E.A., Pascarelle, S., Impey, C., & Petry, C. 1999, ApJ, 511, L4

Francis, P.J., Hewett, P.C., Foltz, C.B., Chaffee, F.H., Weymann, R.J. & Morris, S.L. 1991, ApJ, 373, 465

Francis, P.J. & Williger, G.M. 1994, ApJ, submitted.

Francis, P.J., Woodgate, B.E. & Danks, A.C. 1997, ApJ, 482, 25

Francis, P.J. et al. 1997, ApJ, 457, 490

Geller, M.J. & Huchra, J.P., 1989, Science, 246, 897

Lewis, I.J. et al. 2002, MNRAS, 333, 279

Møller, P., & Fynbo, J. U. 2001, A&A, 372, L57

Palunas, P., Teplitz, H.I., Francis, P.J., Williger, G.M. & Woodgate, B.E. 2004, ApJ 602, in press.

Steidel, C.C., Adelberger, K.L., Shapley, A.E., Pettini, M., Dickinson, M, & Giavalisco, M. 2000, ApJ, 532, 170

This manuscript was prepared with the AAS LaTeX macros v5.0.

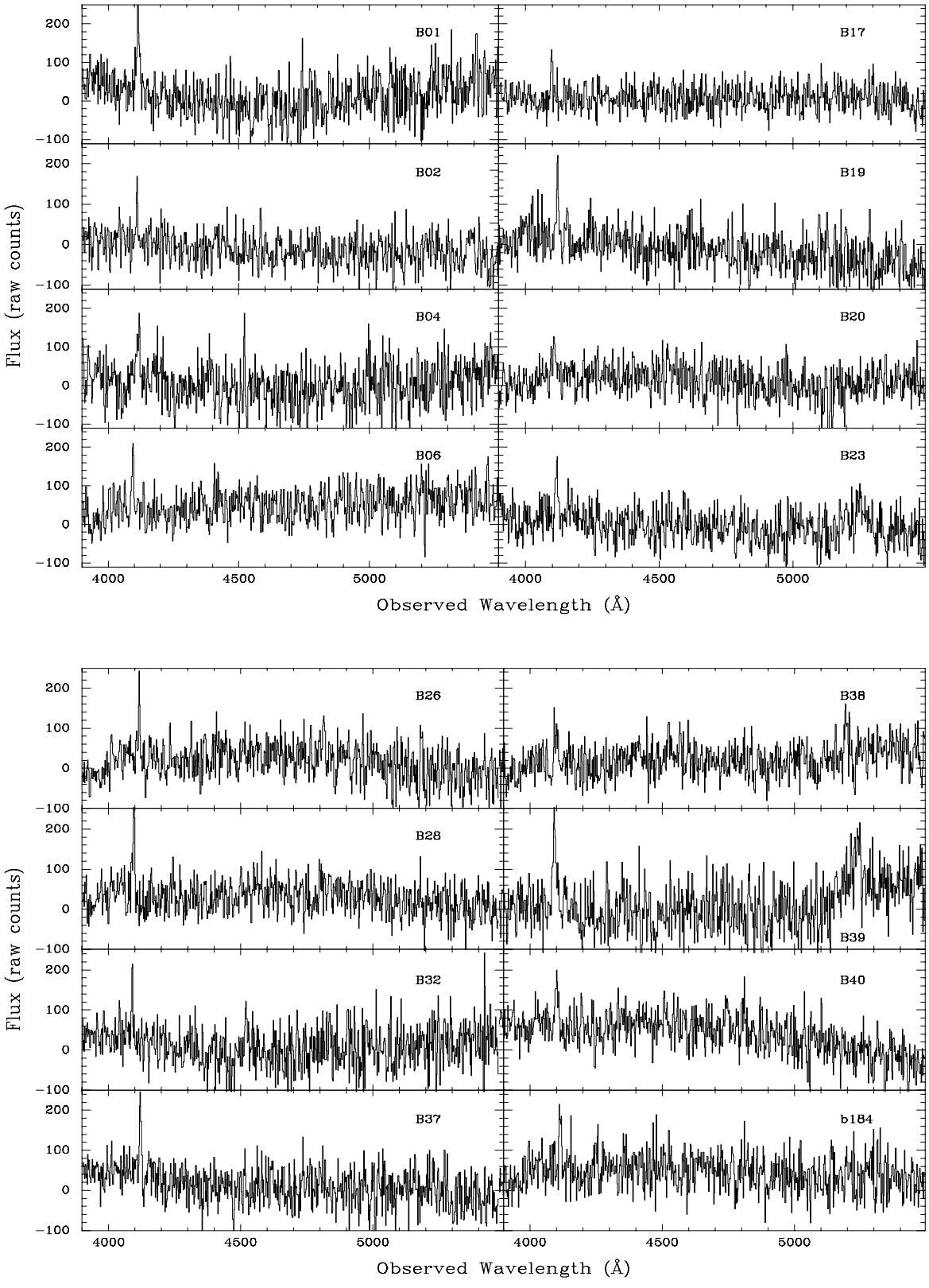

Fig. 1.— Spectra of confirmed ($> 5\sigma$) z=2.38 Lyα emitting galaxies.

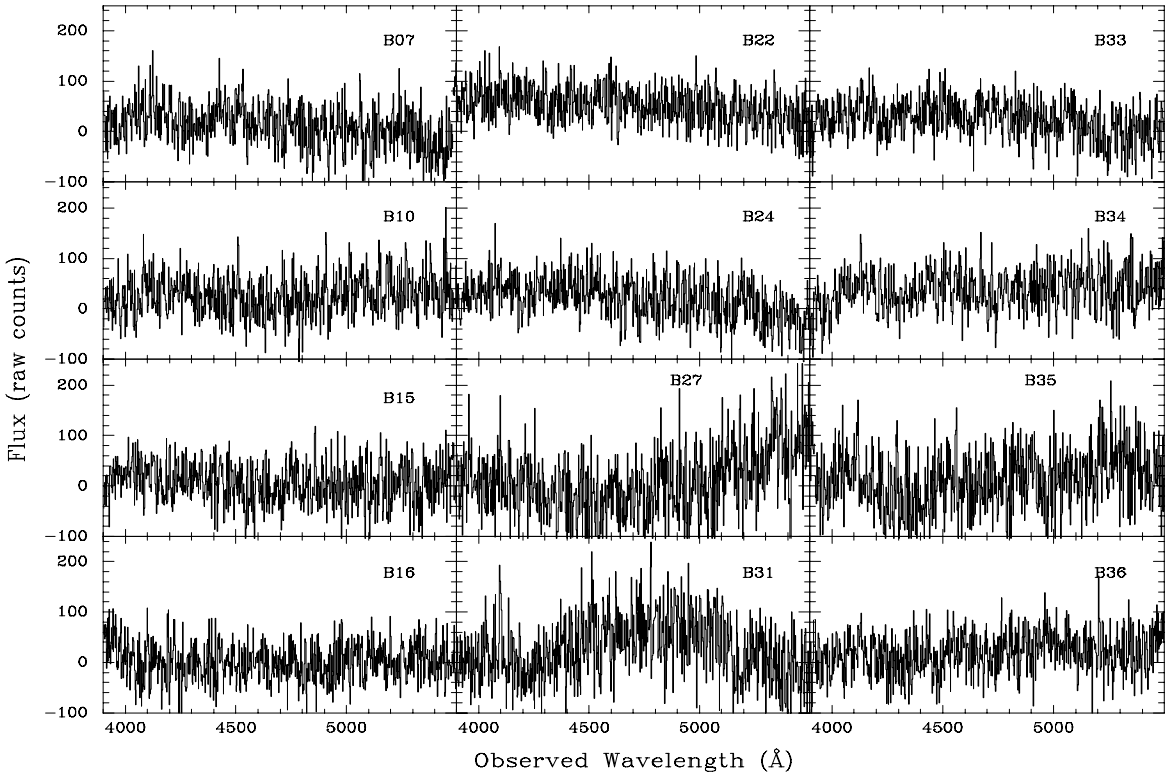

Fig. 2.— Spectra of the marginal (3 – 5 σ) z=2.38 Lyα emitting galaxy candidates.

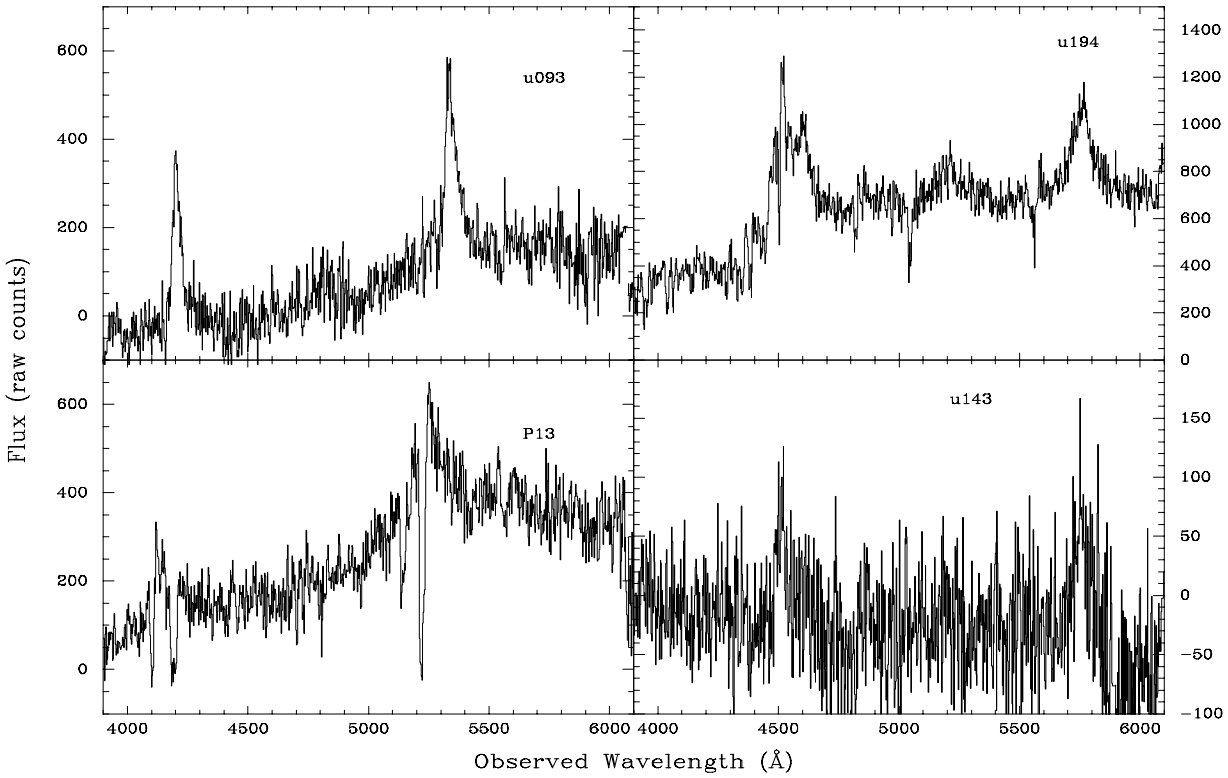

Fig. 3.— Spectra of QSOs lying at or behind the filament redshift.

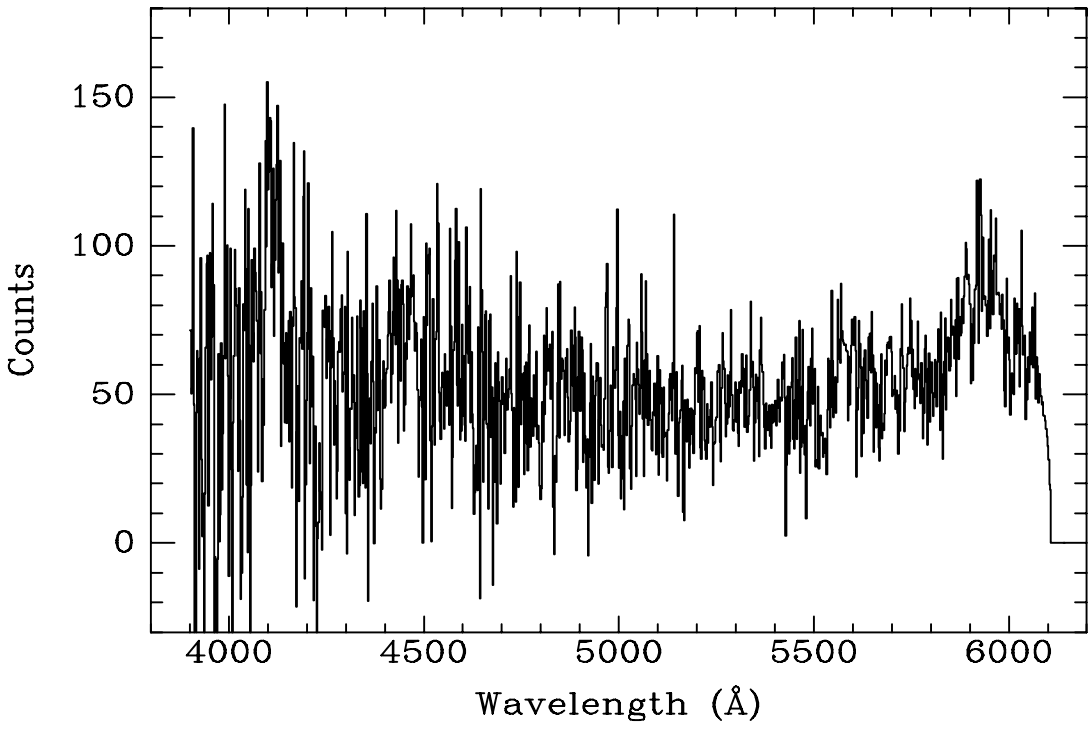

Fig. 4.— Spectrum of B5

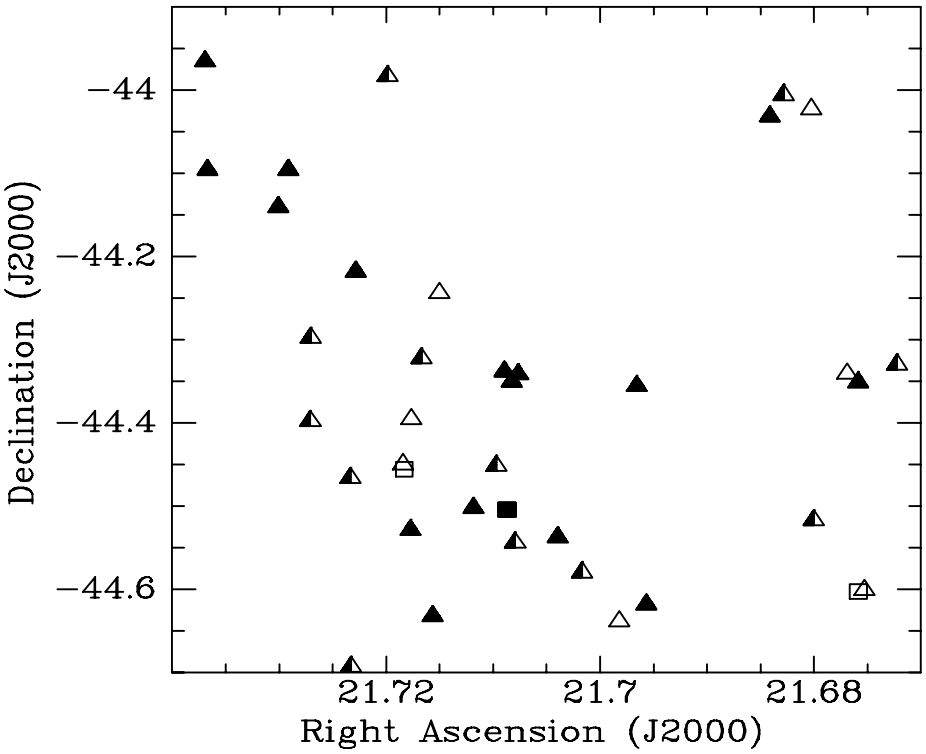

Fig. 5.— Distribution of candidate Lyα emitting galaxies on the sky. Objects with secure spectral confirmations are plotted as solid triangles. Marginal confirmations are shown as half filled triangles, while objects with featureless spectra are empty triangles. The two unobserved candidates are shown as empty squares, and the QSO at the filament redshift as a filled square.

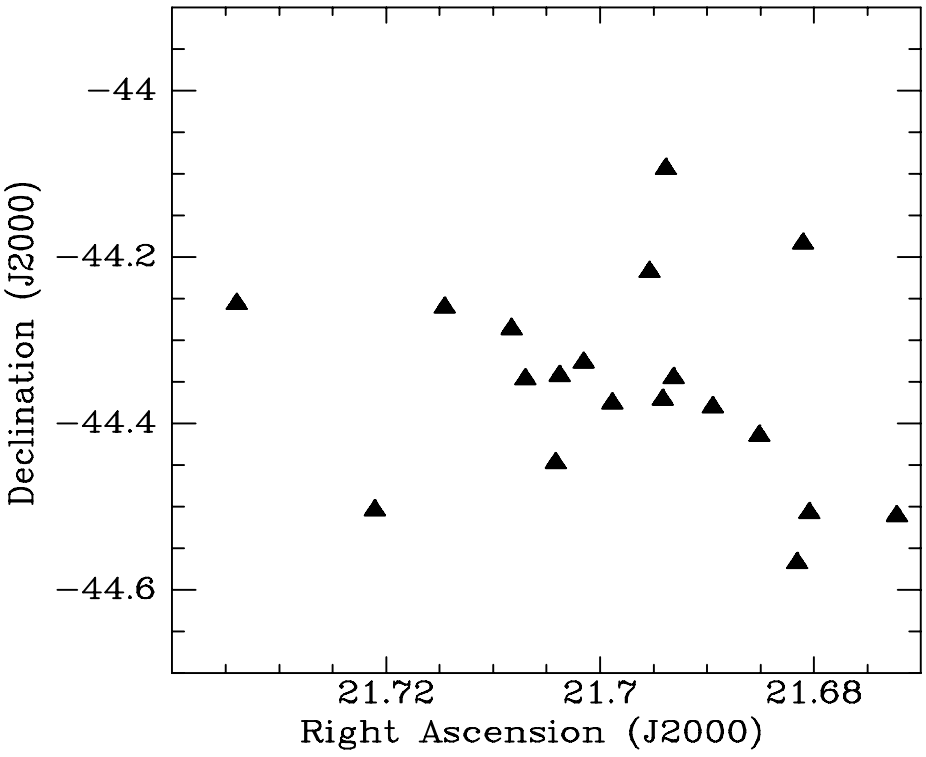

Fig. 6.— Distribution of foreground $z \sim 0.1$, [O II] emitting galaxies in the field.

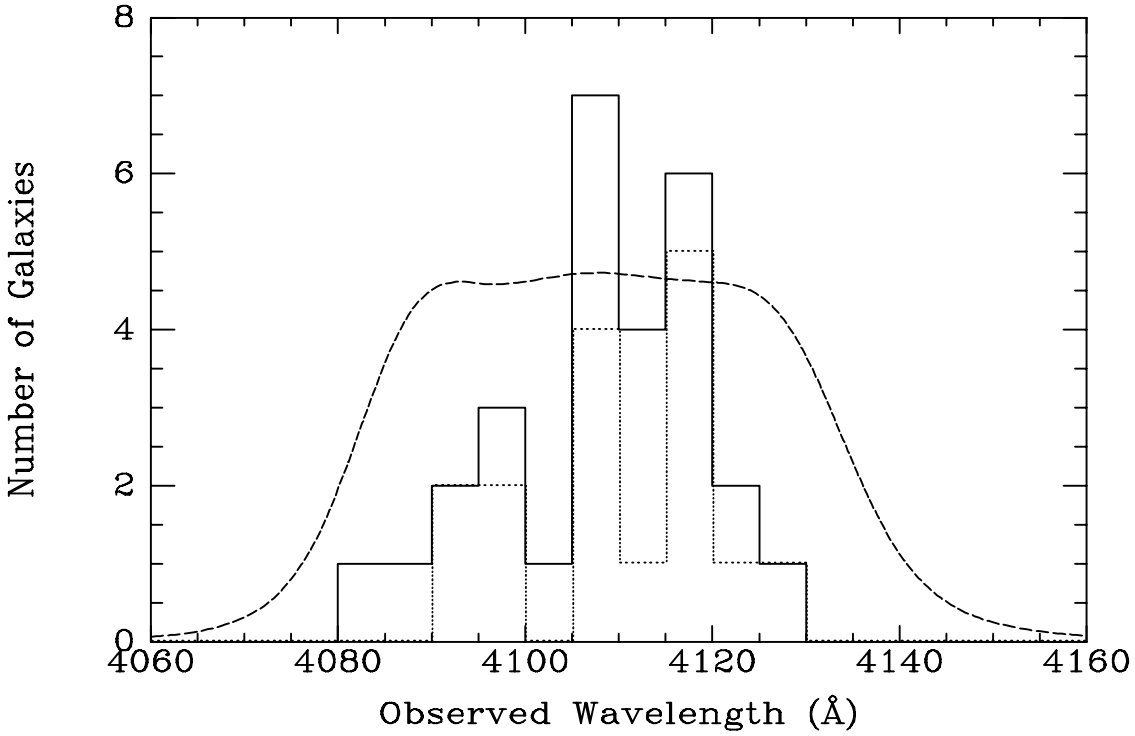

Fig. 7.— Distribution of wavelengths of the secure and marginal Lyα emitting galaxies (solid line) and confirmed sources only (dotted line, slightly offset for clarity), compared to the filter response curve of our narrow-band filter (dashed line), shifted and broadened as appropriate when placed in the converging beam at CTIO prime focus.

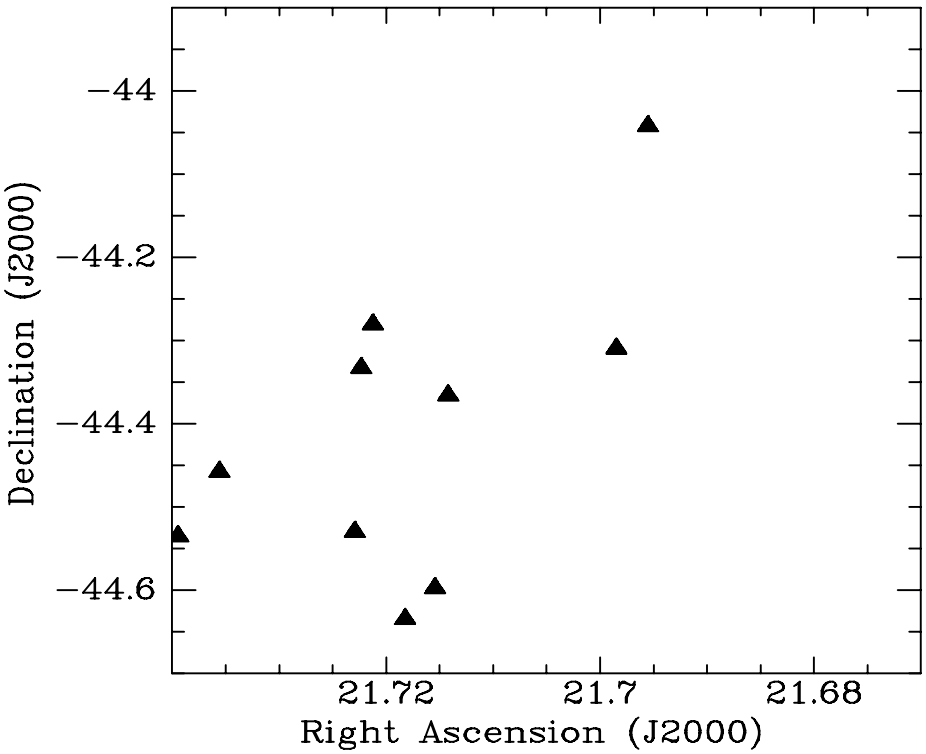

Fig. 8.— Distribution of foreground $1.61 < z < 1.69$ QSOs (QSOs whose C IV line lies within the narrow-band filter passband).

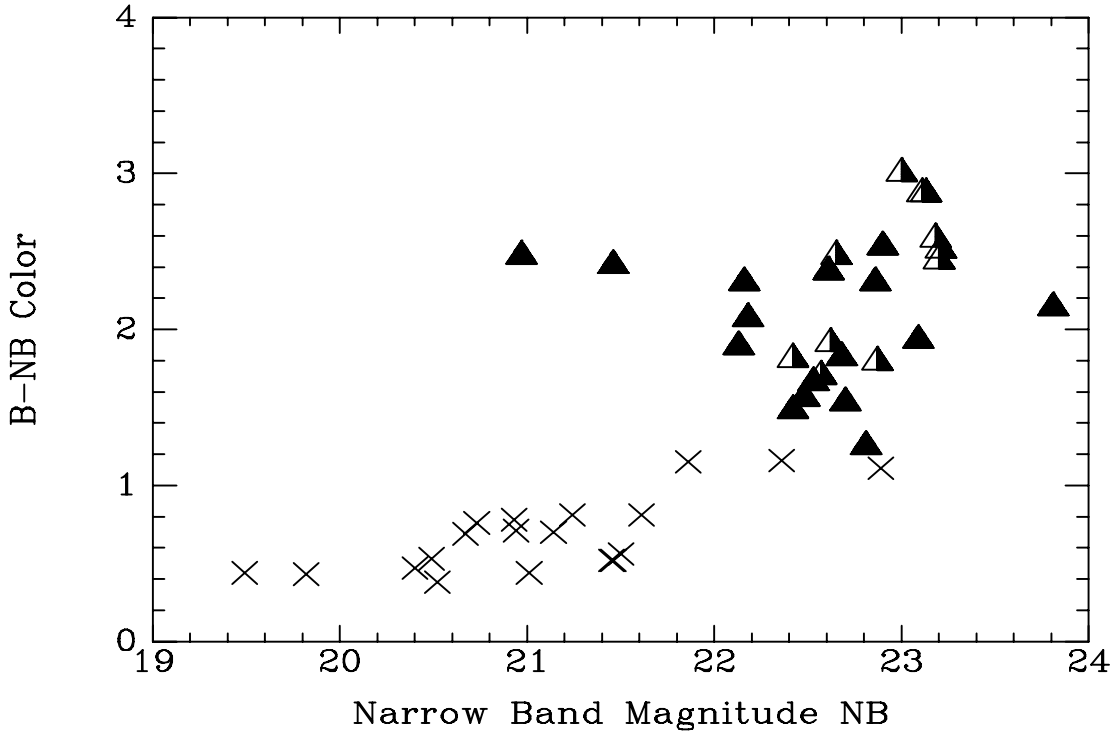

Fig. 9.— The distribution of Broad-band minus narrow-band (B-NB) colors of confirmed Lyα emitting galaxies (filled triangles), marginal Lyα emitting galaxies (half-filled triangles) and confirmed [O II] emitting foreground galaxies (crosses).

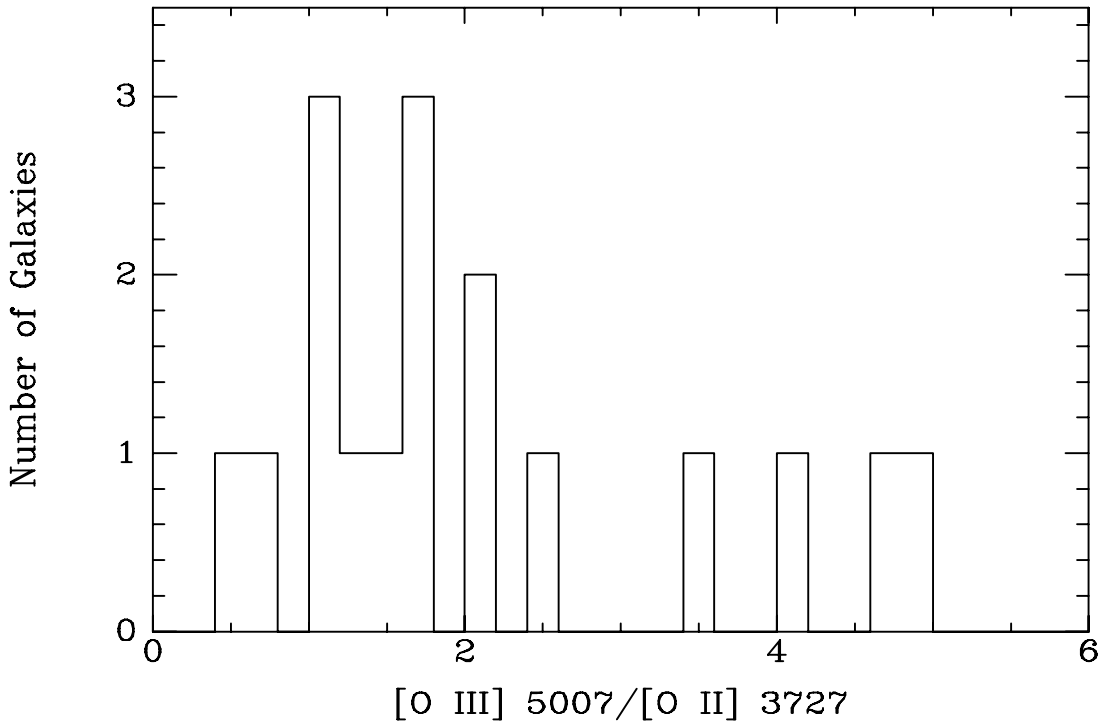

Fig. 10.— The ratio of the flux in the [O III] 5007Å line to that in the [O II] 3727Å line for all foreground galaxies with redshifts placing [O II] in our narrow-band filter bandpass.

Table 1. Confirmed ($> 5\sigma$) Lyα Emitting Galaxies at z=2.38

Name	Lyα Wavelength	Position (J2000)	NB (mag)	B−NB (mag)	FWHM Lyα km s^{-1}
B1	4113	21:42:27.56 -44:20:30.1	20.97	2.47	900
B2	4109	21:42:29.73 -44:21:02.7	22.86	2.30	<450
B4	4117	21:42:32.20 -44:20:18.6	22.90	2.53	1300
B6	4094	21:42:42.63 -44:30:09.0	22.13	1.89	650
B17	4097	21:42:42.63 -44:30:09.0	22.13	1.89	650
B19	4119	21:42:42.63 -44:30:09.0	22.13	1.89	730
B20	4105	21:41:47.66 -44:21:21.9	22.61	2.37	1200
B23	4116	21:42:14.28 -44:32:15.8	22.18	2.07	700
B26	4117	21:42:56.34 -44:37:56.8	22.48	1.56	<450
B28	4097	21:43:03.80 -44:31:44.9	22.16	2.30	730
B32	4090	21:43:03.80 -44:31:44.9	22.16	2.30	<450
B37	4122	21:43:44.92 -44:05:46.3	22.53	1.66	510
B38	4107	21:43:44.92 -44:05:46.3	22.53	1.66	1400
B39	4106	21:44:12.15 -44:05:46.6	21.46	2.41	880
B40	4116	21:44:12.15 -44:05:46.6	21.46	2.41	1160
b184	4129	21:44:12.15 -44:05:46.6	21 46	2.41	870

Table 2. Possible Lyα Emitting Galaxies at z=2.38 (3 – 5 σ)

Name	Lyα Wavelength	Position (J2000)	NB (mag)	B−NB (mag)
B7	4118	21:44:12.15 -44:05:46.6	21.46	2.41
B10	4082	21:40:19.98 -44:19:48.1	22.62	1.91
B15	4121	21:40:19.98 -44:19:48.1	22.62	1.91
B16	4101	21:40:19.98 -44:19:48.1	22.62	1.91
B22	4107	21:42:06.03 -44:34:47.8	23.18	2.58
B24	4087	21:42:06.03 -44:34:47.8	23.18	2.58
B27	4106	21:43:00.09 -44:19:21.7	22.57	1.70
B31	4110	21:43:11.48 -43:59:01.0	23.13	2.87
B33	4111	21:43:23.80 -44:41:36.4	22.87	1.79
B34	4110	21:43:24.06 -44:27:59.9	22.42	1.81
B35	4097	21:43:37.41 -44:17:53.4	23.21	2.51
B36	4109	21:43:37.47 -44:23:52.8	22.65	2.47

Table 3. QSOs

Position (J2000)	Redshift	B mag	Comment
21:40:13.40 -44:09:18.7	2.045	20.78	
21:40:20.82 -44:32:53.1	1.863	20.69	
21:40:28.71 -43:57:06.9	0.793	20.82	1 liner
21:40:30.12 -44:26:06.3	0.608	22.37	1 liner
21:40:34.91 -44:06:48.3	0.461	23.35	
21:40:39.08 -44:03:07.6	2.097	20.31	
21:40:52.48 -44:36:21.5	0.457	19.96	
21:41:12.32 -44:18:25.7	0.692	22.48	1 liner
21:41:13.25 -44:07:38.3	0.742	21.61	1 liner
21:41:13.67 -43:59:53.9	0.688	22.90	1 liner
21:41:15.43 -43:56:00.7	2.202	21.51	
21:41:18.90 -44:20:42.3	0.714	22.93	1 liner
21:41:22.88 -44:06:48.8	2.106	19.95	
21:41:23.97 -44:33:01.3	0.630	20.27	1 liner
21:41:32.62 -44:25:23.4	0.988	21.35	1 liner
21:41:43.91 -44:02:33.9	0.620	20.06	
21:41:54.51 -44:18:36.2	1.647	20.14	
21:41:54.94 -44:42:00.8	2.224	21.89	
21:41:55.73 -44:21:37.4	0.904	20.96	1 liner
21:41:57.61 -44:19:58.8	1.429	20.91	1 liner

Table 3—Continued

Position (J2000)	Redshift	B mag	Comment
21:42:04.05 -44:20:12.5	1.039	21.28	1 liner
21:42:04.90 -44:24:57.5	1.079	19.13	
21:42:07.67 -44:03:10.1	1.732	19.38	
21:42:18.59 -44:08:20.3	1.722	22.88	?
21:42:18.76 -44:15:48.4	1.310	22.00	?
21:42:20.67 -43:59:20.0	2.458	21.59	Background
21:42:21.83 -43:58:11.2	1.112	22.72	?
21:42:25.04 -44:40:02.4	1.458	20.30	?
21:42:29.03 -43:58:38.6	1.853	21.96	
21:42:31.33 -44:30:16.8	2.388	21.24	Filament member
21:42:35.13 -44:32:30.6	0.850	22.34	1 liner
21:42:38.71 -44:06:39.0	1.736	21.10	
21:42:39.38 -44:31:15.2	2.036	22.79	
21:42:43.51 -44:14:25.5	1.589	20.14	
21:42:43.93 -44:32:50.8	1.849	21.44	
21:42:51.15 -44:21:58.9	1.683	21.32	
21:42:51.50 -44:30:43.2	1.795	20.26	
21:42:55.56 -44:35:52.9	1.639	19.51	
21:43:05.59 -44:38:06.6	1.638	20.31	
21:43:11.46 -44:16:20.2	0.664	22.76	1 liner

Table 3—Continued

Position (J2000)	Redshift	B mag	Comment
21:43:12.34 -44:03:35.4	0.984	20.06	
21:43:16.46 -44:16:51.7	1.673	21.71	
21:43:20.40 -44:20:00.5	1.619	21.05	
21:43:20.56 -44:04:25.3	1.044	21.62	1 liner
21:43:22.55 -44:31:49.4	1.631	20.86	
21:43:23.39 -44:35:24.0	2.725	22.02	Background
21:43:23.56 -43:56:38.6	2.223	21.82	
21:43:24.21 -44:04:52.0	1.045	19.44	
21:43:29.62 -44:10:11.9	1.768	21.71	
21:43:32.94 -43:56:31.3	1.557	19.65	
21:43:37.66 -44:08:01.5	2.166	22.02	
21:43:48.73 -44:15:25.1	1.305	22.36	1 liner
21:43:51.26 -44:06:09.6	1.218	22.36	?
21:44:08.11 -44:27:29.8	1.688	20.08	
21:44:17.56 -44:07:02.0	2.725	21.04	Background
21:44:20.92 -44:23:49.8	2.162	20.49	
21:44:22.04 -44:32:07.9	1.648	20.13	
21:44:29.09 -44:12:03.4	2.140	22.86	

Table 4. Foreground Galaxies

Position (J2000)	Redshift
21:40:20.15 -44:30:41.9	0.101
21:40:32.69 -44:32:01.2	0.053
21:40:42.82 -44:12:14.6	0.145
21:40:49.58 -44:30:29.2	0.102
21:40:51.69 -44:11:03.5	0.097
21:40:58.13 -44:22:37.6	0.158
21:41:03.10 -44:17:54.0	0.349
21:41:06.21 -44:12:38.0	0.204
21:41:06.42 -44:24:54.8	0.099
21:41:08.66 -44:30:49.1	0.357
21:41:10.20 -44:29:21.5	0.055
21:41:19.34 -44:12:56.5	0.062
21:41:22.07 -44:22:51.2	0.104
21:41:34.76 -44:02:12.1	0.353
21:41:35.24 -44:20:45.5	0.097
21:41:37.88 -44:05:40.3	0.102
21:41:37.99 -44:29:43.8	0.094
21:41:38.90 -44:22:18.8	0.103
21:41:43.34 -44:13:06.1	0.102
21:41:48.01 -44:16:15.8	0.317

Table 4—Continued

Position (J2000)	Redshift
21:41:48.28 -44:17:34.1	0.328
21:41:54.00 -44:14:29.3	0.055
21:41:55.90 -44:22:34.8	0.094
21:42:02.79 -44:14:44.2	0.311
21:42:05.50 -44:19:38.5	0.102
21:42:12.15 -44:14:53.7	0.566
21:42:13.63 -44:20:35.2	0.099
21:42:14.27 -44:29:11.3	0.264
21:42:14.95 -44:26:53.1	0.099
21:42:25.12 -44:20:50.3	0.098
21:42:25.39 -44:10:40.7	0.406
21:42:29.36 -44:03:27.7	0.470
21:42:29.82 -44:17:12.8	0.099
21:42:40.54 -44:22:22.7	0.562
21:42:40.97 -43:58:15.5	0.510
21:42:51.39 -43:58:16.6	0.137
21:42:52.30 -44:15:40.2	0.101
21:42:56.55 -43:59:23.5	0.143
21:43:06.10 -43:59:04.2	0.462
21:43:15.81 -44:30:17.3	0.100

Table 4—Continued

Position (J2000)	Redshift
21:43:27.59 -44:27:52.0	0.420
21:43:34.40 -44:42:55.6	0.038
21:44:02.26 -44:15:24.1	0.100